

Adequacy of Approximations in GW Theory

Mark van Schilfgaarde,¹ Takao Kotani,¹ and S. Faleev²

¹*Arizona State University, Tempe, AZ, 85284*

²*Sandia National Laboratories, Livermore, CA 94551*

(Dated: February 8, 2020)

Abstract

We use an all-electron implementation of the GW approximation to analyze several possible sources of error in the theory and its implementation. Among these are convergence in the polarization and Green's functions, the dependence of QP levels on choice of basis sets, and differing approximations for dealing with core levels. In all GW calculations presented here, G and W are generated from the local-density approximation (LDA), which we denote as the $G^{\text{LDA}}W^{\text{LDA}}$ approximation. To test its range of validity, the $G^{\text{LDA}}W^{\text{LDA}}$ approximation is applied to a variety of materials systems. We show that for simple sp semiconductors, $G^{\text{LDA}}W^{\text{LDA}}$ always underestimates bandgaps; however, better agreement with experiment is obtained when the self-energy is not renormalized, and we propose a justification for it. Some calculations for Si are compared to pseudopotential-based $G^{\text{LDA}}W^{\text{LDA}}$ calculations, and some aspects of the suitability of pseudopotentials for GW calculations are discussed.

Even though the GW approximation of Hedin¹ is as old as the local-density approximation (LDA), it is still in its early stages because of serious difficulties in its implementation. There have recently arisen two controversies regarding approximations made in the GW theory. Both were raised in a recent Comment by Delaney et. al.², in a criticism of a self-consistent GW approach developed by Ku and Eguiluz³. Both have important implications for the GW community.

The first point concerns the suitability of pseudopotentials (PP) for GW calculations. Substitution of the core with a pseudopotential has been enormously successful in the case of the LDA, and has become ubiquitous. Use of pseudopotentials considerably simplifies computation of matrix elements of the LDA Hamiltonian; similar advantages apply to more advanced theories such as the GW approximation. However, there is to date much less justification for their application to GW theory than there is for LDA, especially for PP constructed from the LDA. Using an all-electron method, we have argued that PP's appear to overestimate semiconductor bandgaps relative to all-electron calculations; Ku made a similar claim for Si³. This has been confirmed by other all-electron methods in cases such as Si^{4,5} or SiC⁵ where the cores are sufficiently deep⁶. We also noted that standard PP's poorly describe the k -dispersion of the conduction band in GaAs⁷, as compared with the all-electron result.

Two recent publications have contested the claim that PP's are not adequate for GW theory. Delaney² showed that GW calculations within the PP approximation produced a reasonable ionization energy for the free Be atom, i.e. it agreed well with an all-electron GW calculation. For the discrepancy between the PP and all-electron gaps in Si noted by Ku³, Tiago and Louie⁸ analyzed the dependence of the gap on the number of unoccupied states n' used to construct the polarization function and self-energy. While we will see that there are several technical details that makes this controversy difficult to answer definitively, this paper presents some analysis of rates of convergence using a recently developed all-electron method⁷, and offers a partial resolution to this controversy. The all-electron method is outlined in Section I, and the convergence is taken up in Section II. Next (Section III) we present results that indicate how this particular kind of analysis—monitoring convergence QP levels as a function of n' —while reasonable, does not characterize the adequacy of a particular basis set for describing QP levels of interest. As part of this analysis, the effect of extensions to the standard energy linearization is considered.

In Section IV we analyze core contributions to the QP levels in several semiconductors to provide some insight as to what approximations can be made concerning the core, and briefly discuss some aspects of the pseudopotential approximation in the GW context (Section V).

The second controversy concerns with the suitability 1-shot GW calculations using the LDA as the potential to generate G and W . We will call this approach $G^{\text{LDA}}W^{\text{LDA}}$. (When pseudopotentials are used in conjunction with $G^{\text{LDA}}W^{\text{LDA}}$ the two approximations cannot be wholly separated.) In Section VI we address this issue by considering a variety of materials systems. We also present an argument supporting the use of an unrenormalized self energy (unit Z factor) in the GW calculation, and show that it significantly improves the $G^{\text{LDA}}W^{\text{LDA}}$ errors in simple sp systems.

I. METHODOLOGY

All-electron LDA

Before turning to the analysis, we briefly describe the basis we use for our GW calculations. The basis functions are generated within the LDA using a generalization⁹ of the standard¹⁰ method of linear muffin-tin orbitals (LMTO). Conventional LMTO's consist of atom-centered envelope functions augmented around atomic sites by a linear combination of radial wave functions φ and their energy derivatives $\dot{\varphi}$. $\varphi = \varphi_{Rl}(\varepsilon_l, r)$ is the solution of radial Schrödinger equation at site R at some linearization energy ε_l . A linear method matches the $\{\varphi, \dot{\varphi}\}$ pair to value and slope of the envelope function at each augmentation sphere boundary, which means that the LDA Schrödinger equation can be solved more or less exactly to first order in $\varepsilon - \varepsilon_l$ inside each augmentation sphere. Envelope functions in the standard LMTO method consist of Hankel functions. In the present basis⁹ the envelope functions are smooth, nonsingular generalizations¹¹ of the Hankel functions: the $l=0$ smooth Hankel satisfies the equation

$$\begin{aligned} (\nabla^2 + \varepsilon)H_0(\varepsilon, r_s; \mathbf{r}) &= -4\pi g_0(r_s, r) \\ g_0(r_s; r) &= (\sqrt{\pi}r_s)^{-3} \exp\left(-r^2/r_s^2\right) \rightarrow \delta(\mathbf{r}) \text{ as } r_s \rightarrow 0 \end{aligned} \tag{1}$$

and reduces to a usual Hankel function in the limit $r_s \rightarrow 0$. H_L for higher $L=(l,m)$ are obtained by recursion¹¹. The basis can be divided into three types of functions:

(i) A muffin-tin orbital χ_{RjL} which consists of a smoothed Hankel centered at nucleus \mathbf{R} and augmented by linear combinations of φ_{Rl} and $\dot{\varphi}_{Rl}$ for each L channel inside every augmentation sphere

$$\chi_{RjL}(\mathbf{r}) = H_L(\varepsilon_j, r_{sj}; \mathbf{r} - \mathbf{R}) + \sum_{R'k'L'} C_{R'k'L'}^{RjL} \{ \tilde{P}_{R'k'L'}(\mathbf{r}) - P_{R'k'L'}(\mathbf{r}) \} \quad (2)$$

$P_{R'k'L'}$ is a one-center expansion of $H_L(\varepsilon_j, r_{sj}; \mathbf{r} - \mathbf{R})$, and $\tilde{P}_{R'k'L'}$ is a linear combination of $\varphi_{Rl}(\varepsilon_l, r)$ and $\dot{\varphi}_{Rl}(\varepsilon_l, r)$ that matches $P_{R'k'L'}$ at the augmentation sphere radius. Expansion coefficients $C_{R'k'L'}^{RjL}$ are chosen to make $\chi_{RjL}(\mathbf{r})$ smooth across each augmentation boundary. ε_l is chosen to be at or near the center of the occupied part of that particular l channel. Augmentation in the LDA requires products of such functions. The present method differs in significant ways from the usual LMTO and LAPW methods, and is not a simple product of muffin-tin orbitals Eq. (2), and bears some resemblance to the Projector Augmented Wave prescription¹². It greatly facilitates l convergence in the augmentation; see Ref. 9.

(ii) “Floating orbitals” which consist of the same kind of function as (i), but not centered at a nucleus. Thus, there is no augmentation sphere where the envelope function is centered. There is no fundamental distinction between this kind of function and the first type, except that the distinction is useful when analyzing convergence. Floating orbitals make little difference in LDA calculations; but a basis consisting of purely atom centered envelope functions is not quite sufficient to precisely represent the interstitial over the wide energy window needed for GW calculations. Without their inclusion, errors in QP levels of order 0.1 eV cannot be avoided, as we will show.

(iii) “Local orbitals” which also have a structure similar to (i). The fundamental distinction is that the “head” (site where the envelope is centered) consists of a new radial function ϕ_l^z evaluated at an energy ε_l^z either far above or far below the linearization energy ε_l . For deep, core-like orbitals ϕ_l^z is integrated at the core energy; for high-lying orbitals ε_l^z is typically taken 1-2 Ry above the Fermi level ε_F . In the former case the smoothing radius r_s is chosen to make the kinetic energy continuous across the “head” augmentation sphere, and thus the local orbital is a precise representation of deep, atomic-like core levels.

As is well known, the reason for using augmented wave methods in general (and especially the LMTO method), is that the Hilbert space of eigenfunctions in the energy range of interest

is spanned by much fewer basis functions than with other basis sets. In the present method two envelope functions $j = 1, 2$ are typically used for low l channels s, p , and d , and one for higher l channels (f and sometimes g). The augmentation + local orbital procedure ensures that the basis is reasonably complete inside each augmentation sphere within a certain energy window; the envelope functions + floating orbitals ensures completeness of the basis in the interstitial. The distinction between standard LMTO envelope functions and the smoothed ones used here is important because the generalized form significantly improves this convergence. Core states not treated as local orbitals are handled by integrating the radial Schrödinger equation inside an augmentation sphere and attaching a smoothed Hankel tail, allowing it to spill into the interstitial. Thus the Hartree and exchange correlation potentials are properly included; only the matrix element coupling core and valence states is neglected.

When used in conjunction with GW calculations we typically add local orbitals for states not spanned by $\{\phi, \dot{\phi}\}$, and whose center of gravity falls within $\sim \pm 25$ eV of the Fermi level. Both the low-lying and high-lying states can be important, and we shall return to it later.

All-electron GW

We briefly describe the present all-electron implementation of the GW approximation. A more detailed account will be given elsewhere¹³. The self-energy is

$$\Sigma(\mathbf{r}, \mathbf{r}', \omega) = \frac{i}{2\pi} \int d\omega' G(\mathbf{r}, \mathbf{r}', \omega + \omega') e^{i\delta\omega'} W(\mathbf{r}, \mathbf{r}', \omega'). \quad (3)$$

In this paper G will be taken to be the one-body non-interacting Green function as computed by the LDA, G^{LDA} , and the RPA screened Coulomb interaction W is computed from G^{LDA} . Both G and W are obtained from the LDA eigenvalues $\varepsilon_{\mathbf{k}n}$ and eigenfunctions $\Psi_{\mathbf{k}n}$. For a periodic hamiltonian, we can restrict \mathbf{r} and \mathbf{r}' to a unit cell and write G as

$$G_{\mathbf{k}}(\mathbf{r}, \mathbf{r}', \omega) = \sum_{n'}^{\text{All}} \frac{\Psi_{\mathbf{k}n'}(\mathbf{r}) \Psi_{\mathbf{k}n'}^*(\mathbf{r}')}{\omega - \varepsilon_{\mathbf{k}n'} \pm i\delta}. \quad (4)$$

The infinitesimal $-i\delta$ is to be used for occupied states, and $+i\delta$ for unoccupied states. W is written as

$$W = \epsilon^{-1} v = (1 - vD)^{-1} v \quad (5)$$

where $D = -iG \times G$ is the bare polarization function shown below, $v = e^2/|\mathbf{r} - \mathbf{r}'|$ is the bare coulomb interaction, and ϵ is the dielectric function.

The quasiparticle (QP) energy $E_{\mathbf{k}n}$ is calculated from perturbation theory

$$E_{\mathbf{k}n} = \epsilon_{\mathbf{k}n} + Z_{\mathbf{k}n} [\langle \Psi_{\mathbf{k}n} | \Sigma(\mathbf{r}, \mathbf{r}', \epsilon_{\mathbf{k}n}) | \Psi_{\mathbf{k}n} \rangle - \langle \Psi_{\mathbf{k}n} | V_{\text{xc}}^{\text{LDA}}(\mathbf{r}) | \Psi_{\mathbf{k}n} \rangle]. \quad (6)$$

$Z_{\mathbf{k}n}$ is the QP renormalization factor

$$Z_{\mathbf{k}n} = \left[1 - \langle \Psi_{\mathbf{k}n} | \frac{\partial}{\partial \omega} \Sigma(\mathbf{r}, \mathbf{r}', \epsilon_{\mathbf{k}n}) | \Psi_{\mathbf{k}n} \rangle \right]^{-1}, \quad (7)$$

and accounts for the fact that Σ is evaluated at the LDA energy rather than the QP energy. Eq.(6) is usually used in GW calculations. As we will discuss later, we present a simple physical argument that indicates using $Z = 1$ is a better choice. However, the results presented here use the Z factor except where noted.

In FP-LMTO, eigenfunctions of the valence states are expanded in linear combinations of Bloch summed muffin-tin orbitals Eq. (2)

$$\Psi_{\mathbf{k}n}(\mathbf{r}) = \sum_{RjL} a_{RjL}^n \chi_{RjL}^{\mathbf{k}}(\mathbf{r}), \quad (8)$$

Core channels are integrated separately as in the LDA; however in the present GW implementation the cores are confined to the augmentation spheres¹⁴. Inside augmentation sphere \mathbf{R} , the Hilbert space of the valence eigenfunction $\Psi_{\mathbf{k}n}(\mathbf{r})$ consists of the pair (or triplet) of orbitals $(\varphi_{Rl}, \dot{\varphi}_{Rl} \text{ or } \varphi_{Rl}, \dot{\varphi}_{Rl}, \varphi_{Rl}^z)$ at that site¹⁵, and can be represented in a compact notation $\{\varphi_{Ru}\}$. u is a compound index for both L and one of the $(\varphi_{Rl}, \dot{\varphi}_{Rl}, \varphi_{Rl}^z)$ triplet. The interstitial is comprised of linear combinations of envelope functions consisting of smooth Hankel functions, which can be expanded in terms of plane waves¹¹. Therefore the $\Psi_{\mathbf{k}n}(\mathbf{r})$ can be written as a sum of augmentation and interstitial parts

$$\Psi_{\mathbf{k}n}(\mathbf{r}) = \sum_{Ru} \alpha_{Ru}^{\mathbf{k}n} \varphi_{Ru}^{\mathbf{k}}(\mathbf{r}) + \sum_{\mathbf{G}} \beta_{\mathbf{G}}^{\mathbf{k}n} P_{\mathbf{G}}^{\mathbf{k}}(\mathbf{r}), \quad (9)$$

where the interstitial plane wave (IPW) is defined as

$$\begin{aligned} P_{\mathbf{G}}^{\mathbf{k}}(\mathbf{r}) &= 0 \quad \text{if } \mathbf{r} \in \text{any MT} \\ &= \exp(i(\mathbf{k} + \mathbf{G}) \cdot \mathbf{r}) \quad \text{otherwise,} \end{aligned} \quad (10)$$

and the $\varphi_{Ru}^{\mathbf{k}}$ are Bloch sums of φ_{Ru}

$$\varphi_{Ru}^{\mathbf{k}}(\mathbf{r}) \equiv \sum_{\mathbf{T}} \varphi_{Ru}(\mathbf{r} - \mathbf{R} - \mathbf{T}) \exp(i\mathbf{k} \cdot \mathbf{T}). \quad (11)$$

\mathbf{T} and \mathbf{G} are lattice translation vectors in real and reciprocal space, respectively.

Through Eq.(9), products $\Psi_{\mathbf{k}_1 n} \times \Psi_{\mathbf{k}_2 n'}$ can be expanded by $P_{\mathbf{G}}^{\mathbf{k}_1 + \mathbf{k}_2}(\mathbf{r})$ in the interstitial region because $P_{\mathbf{G}_1}^{\mathbf{k}_1}(\mathbf{r}) \times P_{\mathbf{G}_2}^{\mathbf{k}_2}(\mathbf{r}) = P_{\mathbf{G}_1 + \mathbf{G}_2}^{\mathbf{k}_1 + \mathbf{k}_2}(\mathbf{r})$. Within sphere R , wave function products can be expanded by $B_{Rm}^{\mathbf{k}_1 + \mathbf{k}_2}(\mathbf{r})$, which is the Bloch sum of the product basis $\{B_{Rm}(\mathbf{r})\}$, which in turn is constructed from the set of products $\{\varphi_{Rm}(\mathbf{r}) \times \varphi_{Rm'}(\mathbf{r})\}$ adapting the procedure by Aryasetiawan¹⁶. Eq. (9) is equally valid in a LMTO or LAPW framework, and eigenfunctions from both types of methods have been used in this GW scheme^{17,18}. We restrict ourselves to LMTO-derived basis functions here.

We define the mixed basis $\{M_I^{\mathbf{k}}(\mathbf{r})\} \equiv \{P_{\mathbf{G}}^{\mathbf{k}}(\mathbf{r}), B_{Rm}^{\mathbf{k}}(\mathbf{r})\}$, where the index $I \equiv \{\mathbf{G}, Rm\}$ classifies the members of the basis. By construction, $M_I^{\mathbf{k}}$ is a good basis set for the expansion of products of $\Psi_{\mathbf{k}n}$. Complete information to calculate Σ and $E_n(\mathbf{k})$ are matrix elements of the products $\langle \Psi_{\mathbf{q}n} | \Psi_{\mathbf{q}-\mathbf{k}n'} M_I^{\mathbf{k}} \rangle$, the LDA eigenvalues $\varepsilon_{\mathbf{k}n}$, the Coulomb matrix $v_{IJ}(\mathbf{k}) \equiv \langle M_I^{\mathbf{k}} | v | M_J^{\mathbf{k}} \rangle$, and the overlap matrix $\langle M_I^{\mathbf{k}} | M_J^{\mathbf{k}} \rangle$. (The overlap matrix of IPW is necessary because $\langle P_{\mathbf{G}}^{\mathbf{k}} | P_{\mathbf{G}'}^{\mathbf{k}} \rangle \neq 0$ for $\mathbf{G} \neq \mathbf{G}'$.) The Coulomb interaction is expanded as

$$v(\mathbf{r}, \mathbf{r}') = \sum_{\mathbf{k}, I, J} |\tilde{M}_I^{\mathbf{k}}\rangle v_{IJ}(\mathbf{k}) \langle \tilde{M}_J^{\mathbf{k}}|, \quad (12)$$

where we define

$$|\tilde{M}_I^{\mathbf{k}}\rangle \equiv \sum_{I'} |M_{I'}^{\mathbf{k}}\rangle (O^{\mathbf{k}})_{I'I}^{-1}, \quad (13)$$

$$O_{I'I}^{\mathbf{k}} = \langle M_{I'}^{\mathbf{k}} | M_I^{\mathbf{k}} \rangle. \quad (14)$$

W and the polarization function D shown below are expanded in the same manner as Eq.(12).

The exchange part of the Σ is written in the mixed basis as

$$\langle \Psi_{\mathbf{q}n} | \Sigma_{\mathbf{x}} | \Psi_{\mathbf{q}n} \rangle = \sum_{\mathbf{k}} \sum_{n'}^{\text{BZ occ}} \langle \Psi_{\mathbf{q}n} | \Psi_{\mathbf{q}-\mathbf{k}n'} \tilde{M}_I^{\mathbf{k}} \rangle v_{IJ}(\mathbf{k}) \langle \tilde{M}_J^{\mathbf{k}} \Psi_{\mathbf{q}-\mathbf{k}n'} | \Psi_{\mathbf{q}n} \rangle. \quad (15)$$

The screened Coulomb interaction $W_{IJ}(\mathbf{q}, \omega)$ is calculated through Eq. (5), where the polarization function D is written

$$\begin{aligned} D_{IJ}(\mathbf{q}, \omega) &= \sum_{\mathbf{k}} \sum_n^{\text{BZ occ}} \sum_{n'}^{\text{unocc}} \langle \tilde{M}_I^{\mathbf{q}} \Psi_{\mathbf{k}n} | \Psi_{\mathbf{q}+\mathbf{k}n'} \rangle \langle \Psi_{\mathbf{q}+\mathbf{k}n'} | \Psi_{\mathbf{k}n} \tilde{M}_J^{\mathbf{q}} \rangle \\ &\times \left(\frac{1}{\omega - \varepsilon_{\mathbf{q}+\mathbf{k}n'} + \varepsilon_{\mathbf{k}n} + i\delta} - \frac{1}{\omega + \varepsilon_{\mathbf{q}+\mathbf{k}n'} - \varepsilon_{\mathbf{k}n} - i\delta} \right). \end{aligned} \quad (16)$$

Eq. (16) assumes time-reversal symmetry. We use the tetrahedron method for the Brillouin zone (BZ) summation in Eq.(16) following Ref. 19. We first calculate the contribution to D proportional to the imaginary part of the second line in Eq. (16), and determine the rest of D by Hilbert transformation (Kramers-Kronig relation). Such approach significantly reduces the computational time required to calculate D .

The correlation part of Σ is

$$\begin{aligned} \langle \Psi_{\mathbf{q}n} | \Sigma_c(\omega) | \Psi_{\mathbf{q}n} \rangle &= \sum_{\mathbf{k}}^{\text{BZ}} \sum_{n'}^{\text{All}} \sum_{IJ} \langle \Psi_{\mathbf{q}n} | \Psi_{\mathbf{q}-\mathbf{k}n'} \tilde{M}_I^{\mathbf{k}} \rangle \langle \tilde{M}_J^{\mathbf{k}} \Psi_{\mathbf{q}-\mathbf{k}n'} | \Psi_{\mathbf{q}n} \rangle \\ &\times \int_{-\infty}^{\infty} \frac{id\omega'}{2\pi} W_{IJ}^c(\mathbf{k}, \omega') \frac{1}{\omega' + \omega - \varepsilon_{\mathbf{q}-\mathbf{k}n'} \pm i\delta}. \end{aligned} \quad (17)$$

Here $-i\delta$ is for occupied states; $+i\delta$ is for unoccupied states. $W^c \equiv W - v$.

GW calculations usually approximate Eq. (6) by

$$E_{\mathbf{k}n} = \varepsilon_{\mathbf{k}n} + Z_{\mathbf{k}n} [\langle \Psi_{\mathbf{k}n} | \Sigma^{\text{Val}}(\mathbf{r}, \mathbf{r}', \varepsilon_{\mathbf{k}n}) | \Psi_{\mathbf{k}n} \rangle - \langle \Psi_{\mathbf{k}n} | V_{\text{xc}}^{\text{LDA}}([n^{\text{Val}}], \mathbf{r}) | \Psi_{\mathbf{k}n} \rangle] \quad (18)$$

where Σ^{Val} and $V_{\text{xc}}^{\text{LDA}}([n^{\text{Val}}])$ refer to the neglect of core contributions. In the present method we calculate $E_{\mathbf{k}n}$ including the core contributions as

$$\begin{aligned} E_{\mathbf{k}n} = \varepsilon_{\mathbf{k}n} + Z_{\mathbf{k}n} \times & [\langle \Psi_{\mathbf{k}n} | \Sigma_x(\mathbf{r}, \mathbf{r}') + \Sigma_c(\mathbf{r}, \mathbf{r}', \varepsilon_{\mathbf{k}n}) | \Psi_{\mathbf{k}n} \rangle \\ &- \langle \Psi_{\mathbf{k}n} | V_{\text{xc}}^{\text{LDA}}([n^{\text{Tot}}], \mathbf{r}) | \Psi_{\mathbf{k}n} \rangle]. \end{aligned} \quad (19)$$

Below we examine the effect of contributions by the core to correlation, and will see that its neglect is quite reasonable except for very shallow cores. Except where stated, the core contribution to Σ_c is left out.

In short, no important approximation is made other than the GW approximation itself; and it is to the best of our knowledge the only implementation of $G^{\text{LDA}}W^{\text{LDA}}$ that makes no significant approximations. Results depend slightly on what kind basis set used to generate G and W , as we will show, and also on the tolerances in parameters used in the GW -specific part of the calculation.

LMTO-based calculations presented here employ a widely varying set of basis functions, ranging from ~ 40 –180 orbitals per atom pair, as described in more detail below. They typically consist of a basis of $spdfg+spd$ orbitals centered on each atom, some floating orbitals and sometimes local orbitals, depending on the calculation. In the Si calculations local p orbitals of either of $2p$ character or of $4p$ character were used, as we describe below. For

the GW part of the calculation, the Si results shown below use parameters representative of the various system studied: LMTO basis functions are expanded in plane waves to a cutoff of 3.3 a.u., i.e. $|\mathbf{k} + \mathbf{G}| < 3.3 \text{ Bohr}^{-1}$ in Eq. (9). The IPW part of the mixed basis used to expand v , D , and W used a cutoff $|\mathbf{k} + \mathbf{G}| < 3.0 \text{ Bohr}^{-1}$; the product basis part consisted of 90–110 Bloch functions/atom (core exchange and valence exchange used different product bases). Augmentation sphere radii were chosen so that spheres approximately touched but did not overlap, and the product basis functions entering into the mixed basis \tilde{M} in Eqns. (16) and (17) were expanded to $l=5$. In the calculation of Eq. (17) the poles of G^{LDA} were Gaussian broadened by $\sigma=0.003$ or 0.01 Ry. These parameters correspond to rather conservative tolerances: tests at tighter tolerances in these parameters change the QP levels by ~ 0.01 eV. (Systematic checks were performed for each material studied.) The linear tetrahedron method was used for D with a $6 \times 6 \times 6$ k -mesh (doubling the number of points in the energy denominator) except where noted. The same mesh is used to calculate D and Σ . This k mesh is reasonably well converged, systematically overestimating conduction-band states by ~ 0.02 eV in Si and similar semiconductors relative to the fully k -converged result.²⁰

II. DEPENDENCE ON CONVERGENCE IN QUASIPARTICLE LEVELS WITH TREATMENT OF χ

We begin by presenting results of several calculations for the Γ_{25v} -X_{1c} gap as a function of the number of unoccupied states n' in Eqns. (16) and (17). In the present section, QP levels are generated from fixed LDA eigenfunctions and eigenvalues, i.e. they are $G^{\text{LDA}}W^{\text{LDA}}$ calculations for a fixed LDA basis. We will show below that analysis of this kind is not the most fruitful way to monitor convergence for efficient basis sets such as the LMTO basis. Such an analysis is nevertheless meaningful provided the basis is complete, and we begin with it because it is customary.

Tiago and Louie⁸ presented a pseudopotential calculation of QP levels in Si, Ge, and GaAs where they included the higher-lying core states into the valence to assess the effect of the core. In the analysis they monitored the rate of convergence in QP levels with n' . They found a slow convergence in n' for the Γ_{25v} -X_{1c} gap, which ostensibly accounts for the discrepancy with Ku's all-electron calculations (which used a rather small n') and their own.

Ku presented a similar analysis²¹, using an LAPW method, and found rapid convergence. Results from both calculations are presented in Fig. 1.

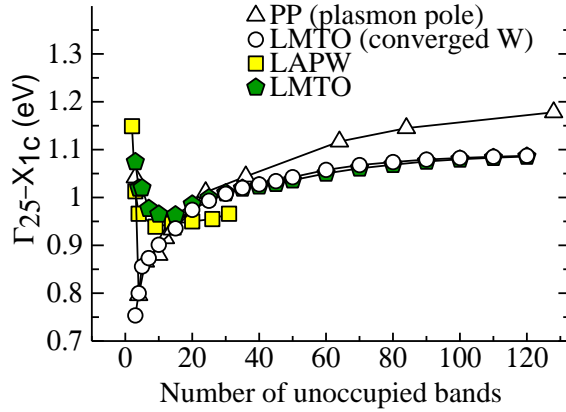


FIG. 1: $\Gamma_{25v}-X_{1c}$ gap in Si, computed by $G^{\text{LDA}}W^{\text{LDA}}$ as a function of the number of unoccupied states n' . Open triangles: PP from Ref. 8. Filled squares: all-electron taken from Ref.²¹, shifted by +0.14 eV to estimate the $\Gamma_{25v}-X_{1c}$ gap from the fundamental gap. Open circles: LMTO results varying n' in G but not W ; filled pentagons: LMTO results varying n' both G and W . LMTO results were shifted by -0.02 eV to correct for incomplete k convergence²⁰.

While Tiago's analysis was reasonable, the true situation appears to be somewhat more complicated, for two reasons. The first has to do with differing treatment of the dielectric function $\epsilon(\mathbf{q}, \omega)$, whose effects are most important for small n' . As is evident from the Figure, LAPW and PP calculations show rather sharply different rates of convergence for small n' (Ku only presented results for $n' \leq 31$). This can be qualitatively understood from the following. The n' -dependence of $\Sigma = iGW$ may be divided into contributions from G and from W : the sum over n' can be truncated independently in Eq. (16) and (17). The former causes the gap to increase with n' . But as n' increases the screening improves, which reduces W and hence the gap. But Because Tiago employed a plasmon-pole approximation, the dependence of W on n' behaves rather differently, as we discuss below.

Squares are Ku's all-electron results, Ref.²¹. Ku presented data for the minimum gap, so we shifted those results by +0.14 eV to estimate the $\Gamma_{25v}-X_{1c}$ gap. Some checks show that the shift should be ~ 0.14 eV, approximately independent of n' .

Open Triangles are data taken from Tiago's PP calculation⁸, which included the Si $2p$ levels as part of the valence. W was computed within the plasmon-pole approximation.

Filled pentagons are results using the present all-electron method when both G and W are allowed to vary. The calculation corresponds to Ku's procedure except that the Si $2p$ core level was included as part of the valence using a local orbital.

Open circles are similar to the filled pentagons, except that W was fixed, as described below.

Filled symbols reflect results from two independent all-electron methods, which avoid the plasmon-pole approximation. It is seen that they track each other reasonably well in the interval where the LAPW data is available ($n' < 31$). The LMTO and LAPW data are shifted by ~ 0.05 eV.

The PP data [triangles] show a radically different behavior for small n' . To see why this might be so, we also include LMTO calculations where W is fixed (i.e. n' is only truncated in Eq. (4)). While the fixed- W and the plasmon pole approximations are obviously not equivalent, there is some correspondence between them, for the following reason. The truncation in n' is equivalent to setting $\text{Im } \epsilon(\mathbf{q}, \omega) = 0$ for large ω ($\omega > \epsilon_{n'} - \varepsilon_F$). $\text{Re } \epsilon(\mathbf{q}, \omega)$ is connected to $\text{Im } \epsilon(\mathbf{q}, \omega)$ through the Kramers-Kronig transformation, consequently the perturbation from truncation in n' is strongest for large ω , and is least affected for small ω . The plasmon pole approximation requires only the static inverse dielectric function; the ω dependence is obtained by assuming $\text{Im } \epsilon^{-1}(\mathbf{q}, \omega)$ has a simple pole structure whose pole is determined by the sum rule. Thus only $\epsilon^{-1}(\mathbf{q}, \omega = \mathbf{0})$ needs to be computed from Eq. (16) (or an equivalent). Because $\epsilon^{-1}(\mathbf{q}, \omega = \mathbf{0})$ depends least on n' , and moreover the sum rule is satisfied by construction, $\epsilon^{-1}(\mathbf{q}, \omega)$ within the plasmon-pole approximation varies much more mildly and smoothly with n' than the true $\epsilon^{-1}(\mathbf{q}, \omega)$. Consequently, a fixed W roughly mimics the plasmon pole approximation. Even if the comparison is not precise, it shows qualitatively how differing treatments of W affects convergence in n' . Comparing filled pentagons (both G and W vary with n') and open circles (only G varies), very different convergence is seen for small n' . As we noted the pentagons reasonably track Ku's results. Since the open circles also reasonably track Tiago's PP plasmon-pole result for small n' , it suggests that at least in this region ($n' < 30$) the sharp discrepancy between the calculations of Ku and Tiago can be attributed to differing treatments of ϵ .

Differing treatments of W affect the n' dependence only for small n' : the difference between pentagons and circles is small for $n' > 20$. Inspection of Fig. 1 suggests that the PP

and LMTO results converge for large n' at similar, but not identical rates. We turn to this point next.

III. CONVERGENCE IN QUASIPARTICLE LEVELS: BASIS DEPENDENCE

While Fig. 1 reveals a band-by-band decomposition of the contribution to Γ -X gap and is therefore meaningful, usually we are only interested in the converged result. For such a purpose we can monitor the convergence with respect to the size of basis in another way, namely by varying n' which for any n' includes the *entire basis* used to expand the eigenfunctions. The difference is significant, as we show below.

In any case, decomposition of QP levels by band as shown in Fig. 1 is not especially meaningful when a small basis is used, i.e. when the number of occupied+unoccupied states is of the same order as the basis dimension (as can easily occur for a method such as the present one), since the basis will not be complete over range of n' . The higher-lying states in such a case do not precisely correspond to individual eigenfunctions of those states. However, it is not necessary that they do so, but only that the basis be sufficiently complete to describe the dynamical response $D = -iG \times G$ between the static limit and time scales that affect the QP levels of interest. From this perspective, the higher-lying states of such a basis may be viewed as a kind of average of the actual unoccupied states and will approximately describe their collective contribution to dynamical response best at low frequencies; the precision will deteriorate with increasing frequency. Alternatively, Eq. (4) should just be regarded merely as device to make G , a quantity that could be obtained by some alternate method (e.g. $G(\omega) = (\omega - H)^{-1}$) which is not computed by summation over separate band contributions. Similarly D need not be generated by the perturbation expression Eq. (16) but could be obtained through $D = iG \times G$. (D can also be calculated in principle via the Sternheimer equation, which involves only occupied states).

As we will see, a basis sufficient for accurate description of the first few unoccupied QP levels is somewhat larger than what is needed for LDA calculations, but nevertheless it can be relatively small. The key point is that there is little relation between convergence in n' using the entire Hilbert space of a small basis, and adopting a large basis and truncating the summation over n' in Eqs. (16) and (17) to a small number. The contrast between these two approaches can also be viewed from another perspective. In the former case the complete

Hilbert space as defined by the basis is used for all parts of the calculation, and it provides a consistent and analytic treatment of the Hilbert space. Truncation in n' , on the other hand, introduces discontinuities in D . G may be thought of as a functional of H ; and generating a different G by truncating n' may be regarded as a functional of a different H' , which would have very different structure, one that is very unsmooth compared to the original H . There is a familiar parallel: Friedel oscillations in the density result from a discontinuous change in single-particle occupation numbers at the Fermi level. The discontinuities are responsible for the slow convergence in QP levels seen in Fig. 1.

Fig. 2 compares the dependence of the Γ_{25v} - X_{1c} gap on n' for relatively small and large basis sets. (An approximate correspondence between the LDA energy $\varepsilon_{\mathbf{k}n'}$ and n' is shown in the top scale in the Figure.) For $n' > 30$, X_{1c} rises much more rapidly with n' in the small-basis case. But QP levels at the respective maximum n' —when n' includes all unoccupied states in each respective Hilbert space—are very similar. This is because both basis sets are sufficiently complete to represent G and D for time scales that affect the lowest QP levels. We show in more detail below that this is not merely an artifact of this particular pair of basis sets.

The n' dependence is also revealing for small n' . LDA eigenvalues $\varepsilon_{\mathbf{k}n'}$ for states up to $\sim \varepsilon_{VBM} + 1.5$ Ry, or $n' \approx 25$, are nearly indistinguishable between the large and small basis sets; and $G^{\text{LDA}}W^{\text{LDA}}$ levels evince a correspondingly similar variation with n' apart from a constant shift of ~ 0.01 eV. In principle, both curves should converge to a common value as n' becomes small. That they deviate slightly is not a measure of convergence in the basis, but is connected with limitations to numerical precision in the method. Between these two basis sets, LDA occupied bands $\varepsilon_{\mathbf{k}n}$ and total energy differ by $\sim 10^{-4}$ and $\sim 10^{-3}$ Ry respectively. The self-consistent LDA density changes slightly with basis set, indicating slight inconsistencies in the eigenfunctions. Thus, even though the LDA levels are nearly identical, $G^{\text{LDA}}W^{\text{LDA}}$ level differ by ~ 0.01 eV even for small n' . This is because the eigenfunctions are represented in very different ways in the two basis sets; and slight inconsistencies in them are responsible for the QP shift. It is not insignificant that the $G^{\text{LDA}}W^{\text{LDA}}$ level is ~ 0.01 eV higher in the small basis case *both* for small n' and at n'_{max} : it is an indication that incompleteness of basis is not the dominant source of the discrepancy between the two basis sets. We will see below that apparently random shifts of order ± 0.01 eV occur (for a fixed choice of $\{\varphi_{Ru}\}$) when comparing a wide variety of basis sets. Similar discrepancies are seen

when comparing to levels generated by an LAPW basis: with similar input conditions for the GW part—similar tolerances and approximately similar augmentation functions $\{\varphi_{Ru}\}$ —the LAPW QP levels fall ~ 0.04 eV higher than those calculated by the present method²². Moreover, there is a slight dependence of QP levels on augmentation radius: shrinking augmentation sphere volume by 30% has the effect of increasing the gap by ~ 0.01 eV. Thus numerical accuracy is limited to order ~ 0.1 eV or a little less for Si.

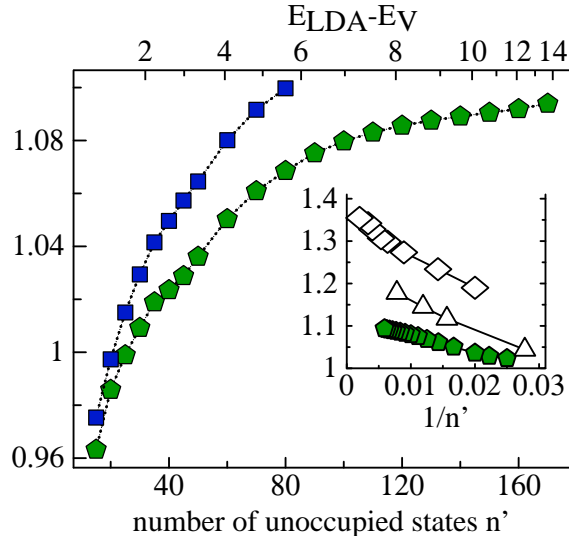


FIG. 2: $\Gamma_{25v} \rightarrow X_{1c}$ gap in Si, as a function of number of unoccupied states n' for a smaller basis (squares) and a larger basis (pentagons). The latter are redrawn from Fig. 1. Top horizontal scale shows an approximate relation between energy and band index (interpolated from levels at Γ in the large basis). Inset compares convergence in X_{1c} as a function of $1/n'$ to a PP calculation that includes $2p$ states in the valence⁸ (triangles) and a PP calculation that does not²³ (diamonds). LMTO data were shifted by -0.02 eV to correct for incomplete k convergence²⁰.

There is an independent, but related issue connected with the Hilbert space of basis functions. A linear method is valid only over a limited energy range. This is true for linear augmented-wave methods, as it is for pseudopotential approaches using standard norm conservation conditions²⁴. Norm-conservation ensures that the radial wave function and its first energy derivative are correctly described for the free atom; higher order energy derivatives are not included properly. Even though a linear all-electron method and a pseudopotential method are not equivalent, they share in common a limitation that eigenfunctions are expanded in a basis that is correct only to linear order about some reference energy.

In the case of Si, the validity of the linear method should extend approximately for $\sim \varepsilon_l \pm 2$ Ry, as determined from standard analysis of potential functions in the LMTO-Atomic Spheres Approximation. Thus we can expect that without extensions to the linear method, the LDA levels are only well characterized for energies below $\sim \varepsilon_l + 2$ Ry, regardless of the basis size. This is a rather wide window, so the errors in a linear approximation are small for Si; but even in this case they are not completely negligible, as we shall see.

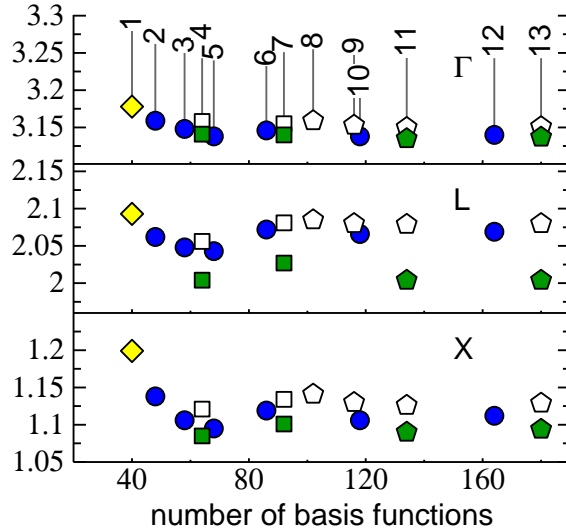


FIG. 3: $G^{\text{LDA}} W^{\text{LDA}}$ calculations of Γ_{15c} (top), L_{1c} (middle), and X_{1c} (bottom) levels in Si relative to the valence band maximum, using different basis sets in the LMTO method. Filled circles denote basis sets using a strictly linear method. Filled(open) squares extend the linear method with the addition of Si $2p(4p)$ local orbitals; filled(open) pentagons denote the further addition of a Si $4d$ local orbital. Data set (1) marked by diamonds consists of $spdfsp$ atom-centered functions, and is the only basis without floating orbitals. Abscissa is the total number of basis functions N ; thus the number of unoccupied states n' is ten less than N for filled squares and pentagons, and four less for all other cases. Sets (2) and (3) contain respectively a minimum (sp) and reasonably converged (spd) set of floating orbitals. The main difference in QP levels for sets (3) and larger can be attributed to contributions from local orbitals.

Fig. 3 shows results of a systematic study of the convergence in the first unoccupied QP levels at Γ , X , and L in Si with progressively larger LDA basis sets. The entire basis is included in the calculation of G and W ; n' changes through changes in the basis. These data comprise very diverse basis sets, particularly for the LMTO method which traditionally uses

a minimal basis. Some details concerning these sets help explain in what manner convergence is reached:

§1 basis set (1)—diamonds—include only envelope functions centered at the two nuclei.

It is the only basis without floating orbitals.

§2 Basis sets (2) and (3) include floating orbitals of *sp* and of *spd* character, respectively.

Their effect is to cause the QP levels to *decrease* slightly relative to (1).

§3 The larger bases (5, 6, 10, 12) add still more envelope functions comprised of a mixture of more atom-centered functions and more floating orbitals.

§4 Basis sets (4, 7, 11, 13)—squares and pentagons—include local orbitals for the *p* state (open symbols includes the Si 4*p* state; filled symbols the 2*p* state). Pentagons include a additional local orbital in the 4*d* channel. Sets (3, 6, 10, 12) correspond to (4, 7 or 8, 11, 13), except that local orbitals are absent and the basis thus corresponds to a strictly linear method. A local orbital of *either* 2*p* or 4*p* character shifts the QP levels—in roughly equal but opposite directions. The effect of the 4*d* channel is small.

§5 Not shown are the corresponding LDA levels. This is because they are the same to within ~ 0.01 eV for all the basis sets shown in the Figure (0.60 eV for X, 1.42 eV for L, 2.52 eV for Γ). This is to be expected because the LDA potential depends only on the occupied states, which are reasonably complete for all the basis sets in the Figure.

These points show in a compelling way that once the basis reaches a certain level of completeness, the change of QP levels with further enlargement is very small. Set (1), which consists only of atom-centered functions, is somewhat incomplete except inside the augmentation spheres where the eigenfunctions are constructed out of linear combinations of $\{\phi, \dot{\phi}\}$. Considering the open structure of zincblende, such a basis may be expected to be less complete in the interstitial. Comparison with sets (2) and (3) show that this particular purely atom-centered basis⁹ is slightly deficient for reliable calculation of *GW* QP levels, since the addition of floating orbitals induces a (*k*-dependent) reduction in the conduction band of $\sim 0.02 - 0.10$ eV. It is an open question whether a still more sophisticated atom-centered basis²⁵ would be adequate to describe the interstitial.

Once the interstitial is reasonably complete (*cf.* sets (3) and higher), there is an almost negligible dependence on basis *provided* no orbitals are included that extend the linear

method or alter how the core is treated. Basis sets marked by a common symbol (squares, circles, pentagons) share essentially the same Hilbert space in the *augmentation* regions; only the basis set corresponding to the *interstitial* region changes. The variation is ± 0.01 eV for a wide range of basis sets. As we noted, the apparently random remaining variations are an artifact of the rather significant change in how eigenfunctions are represented as the basis changes. This is apparently a drawback to the present method as compared to plane-wave methods, where representations of eigenfunctions change smoothly as the basis is enlarged.

Fig. 3 also gives us some insight to the limitations of the linear method. Basis sets (3) and (4), which differ only in how the Si p channel is treated inside the augmentation region, affect the QP levels more strongly than radically enlarging the Hilbert space of the envelope functions—compare (3)→(4) and (3)→(12). Envelope functions affect only the interstitial; they negligibly affect the Hilbert space of the augmentation region. For the latter it is largely irrelevant how many envelope functions are used—and consequently the size of n' entering into Eqns. (16) and (17)—what is relevant is the completeness of $\{\phi, \dot{\phi}\}$, and that the entire $\{\phi, \dot{\phi}\}$ Hilbert space be included. Said another way, the LMTO method is designed to have a reasonably complete Hilbert space over a certain energy window in the augmentation spheres. A similar story may be told for the interstitial: sets (3, 6, 10, 12) differ in the number of envelope functions by as much as a factor of three, but QP levels are unchanged within ± 0.01 eV. The QP levels shift when $\{\phi, \dot{\phi}\} \rightarrow \{\phi, \dot{\phi}, \phi^{4p}\}$ or $\{\phi, \dot{\phi}\} \rightarrow \{\phi, \dot{\phi}, \phi^{2p}\}$, essentially independently of the number of envelope functions (3→4, 6→7, 10→11, 12→13).

Table I shows three examples in addition to Si where there is (1) rapid convergence in the QP levels as the basis is enlarged for a *fixed* set of augmentation functions and (2) extensions to a linear augmentation affect the QP levels in an manner approximately independent of the total dimension of the Hamiltonian. (In GaAs omitting either the $3d$ or the $4d$ orbitals is a poor approximation; neglecting one or the other results in significant errors⁷). We have tested a number of other materials as well, and these trends appear to be rather general. As might be expected, the number of basis functions needed to make the Hilbert space reasonably complete depends somewhat on the elements involved. The heavier atoms have larger radii and consequently slower l -convergence in the number of envelope functions needed; also d orbitals often play an important role. More orbitals are required to make the basis complete when heavier atoms are involved.

As noted, the linear $\{\phi, \dot{\phi}\}$ Hilbert space is already reasonably complete in the case of Si.

TABLE I: QP levels of the first unoccupied state at Γ , L, and X, for different basis sets, in eV. Columns n_a , n_f , and n_l denote the number of atom-centered functions, the number of floating orbitals, and the number of local orbitals respectively. The hamiltonian dimension is the sum of these numbers. Experimental data are adjusted for spin-orbit coupling by adding 1/3 of the splitting in the Γ_{15} valence bands, as calculated within the LDA including spin-orbit coupling. The first four CdO basis sets are identical to the last four except for the addition of local orbitals in the O 3p and Cd 5d channels. A $6 \times 6 \times 6$ k -mesh was used in these calculations.

Data type	n_a	n_f	n_l	Γ	L	X
CdO						
Expt+0				0.84		
LDA	59	18	12	-0.53	4.26	3.58
$G^{\text{LDA}}W^{\text{LDA}}$	59	18	12	0.14	5.18	4.97
	59	50	12	0.10	5.14	4.92
	82	66	12	0.10	5.16	4.89
	82	82	12	0.10	5.16	4.88
	59	18	3	-0.01	5.05	4.78
	59	50	3	-0.06	5.01	4.73
	82	66	3	-0.02	5.05	4.73
	82	82	3	-0.02	5.06	4.74
Ge						
Expt+0.10				1.00	0.88	1.20
LDA	50	18	10	-0.12	0.07	0.65
$G^{\text{LDA}}W^{\text{LDA}}$	50	18	10	0.80	0.65	0.94
	68	18	10	0.84	0.68	0.97
	82	50	10	0.83	0.67	0.96
	82	82	10	0.82	0.67	0.96
GaAs						
Expt+0.11				1.63	1.96	2.11
LDA	42	18	6	0.34	0.86	1.34
$G^{\text{LDA}}W^{\text{LDA}}$	42	18	6	1.44	1.68	1.79
	68	18	6	1.46	1.69	1.79
	82	50	6	1.44	1.66	1.77
	82	82	6	1.43	1.66	1.77
	82	82	11	1.43	1.68	1.81

But this is not true in general: oxides and nitrides form a materials class where the effect is significantly larger. CdO is one such example (CdO forms in the NaCl structure; the valence band maximum falls at L and the conduction band minimum falls at Γ .) As happens for Si, there is a weak dependence on basis when the number of envelope functions is changed and the Hilbert space of the augmentation is held constant. But the QP levels change by $\sim 0.15 \pm 0.05$ eV when the O 3p and Cd 5d states are added, as Table I shows. (In this particular case it is the O 3p contribution that is dominant; however, cases arise when the contributions from high-lying *d* or *f* orbitals can be of order 1 – 2 eV. NiO is such a case²⁶.)

IV. CORE CONTRIBUTIONS

In a series of papers, Shirley and co-workers analyzed the effects of the core on QP levels in atoms^{27,28} and semiconductors^{29,30} within the pseudopotential framework. Approximate core contributions to both Eq. (16) and (17) were evaluated to correct standard pseudopotential treatment of the core. Shirley also compared pseudopotentials constructed from both LDA exchange and from Hartree-Fock (HF) exchange for atoms and molecules³¹, and incorporated pseudopotentials of both types in studying core effects^{29,30}. He found sizeable shifts in QP levels in Si, and rather dramatic and *k*-dependent shifts in Ge and GaAs.

Shirley's analysis highlights the importance of core effects. His analysis is somewhat involved, and it is rather closely tied to the pseudopotential construction that was a part of his implementation. This makes it a little difficult to disentangle the various contributions, and so we consider here an all-electron approach, where the entire $V_{\text{xc}}^{\text{LDA}}$ is subtracted (Eq. (19)); thus $V_{\text{xc}}^{\text{LDA}}$ enters only in the construction of $\Psi_{\mathbf{k}n}(\mathbf{r})$ and $\varepsilon_{\mathbf{k}n}$ used to make G and D . We showed previously⁷ that computing QP levels by subtracting only $V_{\text{xc}}^{\text{LDA}}[n^{\text{Val}}]$ — i.e. computing QP levels though Eq. (18)—is a poor approximation, and indeed it is disastrous in GaAs.

Dividing Σ into an exchange part and a correlation part, $\Sigma - V_{\text{xc}}^{\text{LDA}} = \Sigma_{\text{x}} + \Sigma_{\text{c}} - V_{\text{xc}}^{\text{LDA}}$, the core contribution to Σ_{c} , Eq. (17), can be evaluated at various levels of approximation. G is readily partitioned into $G = G^{\text{Val}} + G^{\text{Core}}$ by partitioning the sum over n' into core and valence states in Eq. (4) or (17). D can be similarly partitioned into $D = D^{\text{Val}} + D^{\text{Core}}$. D generates W through Eq. (5) and therefore the correlation potential $W^{\text{c}} = W[D] - v$ can be partitioned into a valence contribution ($W[D^{\text{Val}}] - v$) plus a residual ($W[D] - W[D^{\text{Val}}]$).

The core contribution to Σ_c , Eq. (17), can then be approximated in one of four ways:

- (i) neglect the core contribution to Σ_c entirely: i.e. approximate G with G^{Val} and W^c with $W[D^{\text{Val}}] - v$. All that remains from the core is its contribution to the Fock exchange Σ_x , as originally proposed by Aryasetiawan. This exchange-only treatment of the core is the lowest level of approximation.
- (ii) Include the core contribution to G but neglect its contribution to W^c
- (iii) Include the core contribution to W^c but neglect its contribution to G in Eq. (17)
- (iv) include the core contribution to both D and G

Independently of this, we can treat the core state explicitly as valence through the use of local orbitals, or solve for the core independently, which leaves out the (LDA) matrix elements coupling core and valence states. For shallow cores with their larger radial extent, approximations in our present treatment of core states¹⁴ do not enable us to distinguish true core contributions from artifacts of the implementation, so we use the local orbital approach here. For a deep core such as the Si $2p$ it matters little whether the core eigenfunctions are computed separately or generated through a local orbital, even with the approximate core treatment¹⁴. This is expected since the core level is very deep. Since the LDA eigenfunctions are represented completely differently in the two cases, the stability is a confirmation of the robustness of the GW implementation.

Table II shows that the difference between exchange-only and GW approximations to core treatment is rather small in Si (~ 0.03 eV for X_{1c}). As expected, the adequacy of an exchange-only core depends on how deep the core is. Shallow cores, such as the Ga $3d$ and In $4d$, and the highest lying p core in the column I (Na, K, Rb) and column IIA alkali metals (Mg, Ca, and Sr), can only be approximated rather crudely at the exchange-only level. (It is interesting that the core contributions to D and to G are *not* always additive. The core contribution to W can affect the core contribution to Σ through G^{Core} ; thus $G^{\text{Core}}(W - W^{\text{Val}})$ can be of the same order as $G^{\text{Core}}W^{\text{Val}}$.

The contribution G^{Core} makes to Σ^c is in general rather small; that is, inclusion of core contributions of D alone is sufficient to bring QP results within 0.05 eV of the full results in Table II except for the very shallow Ga $3d$ channel. For moderately deep cores, exchange-only treatment of cores is generally adequate, as Aryasetiawan first suggested. A rough rule

TABLE II: QP levels of the first unoccupied state at Γ , L, and X relative to top of valence, for core treatments (i) – (iv) as described in the text, in eV. Core levels $\varepsilon_c^{\text{LDA}}$ are: 2p in Si, 3d in Ga and Ge, and 2s in Mg. Si data corresponds to basis set (13) in Fig. 3; GaAs data corresponds to the 68+18+6–orbital basis in Table I; Ge data corresponds to the 68+18+10–orbital basis in that table. A $6 \times 6 \times 6$ k -mesh was used in these calculations.

	$\varepsilon_c^{\text{LDA}}$	$G^{\text{Val}}, W[D^{\text{Val}}]$			$G, W[D^{\text{Val}}]$			G^{Val}, W			G, W		
		Γ	L	X	Γ	L	X	Γ	L	X	Γ	L	X
Si	-89.6	3.17	2.09	1.14	3.17	2.09	1.14	3.17	2.06	1.15	3.16	2.02	1.11
Ge	-24.7	0.98	0.74	0.98	0.96	0.73	0.95	0.88	0.71	0.99	0.84	0.68	0.97
GaAs	-14.8	1.65	1.83	1.86	1.63	1.82	1.85	1.54	1.75	1.83	1.46	1.69	1.79
MgO	-71.4	7.31	10.55	11.62	7.36	10.56	11.62	7.30	10.55	11.60	7.36	10.55	11.60

of thumb seems to be: for cores whose total charge outside the augmentation radius is less than 0.01 electrons, exchange-only treatment of them results in errors ~ 0.1 eV or less for the lowest excited states. (This radius may be taken as approximately half the nearest-neighbor bond length).

Inclusion of core contributions D^{Core} and G^{Core} can significantly increase the computational cost (in the case of Si, leaving out the 2p contribution to D reduces the computational cost by $\sim 40\%$). The relative smallness of corrections to exchange-only treatment, and the observation that core contributions to D alone are adequate for all but the most shallow cores, suggests that a simple approximate inclusion of core contributions to D , Eq.(16), should be adequate for all but the most shallow cores such as the Ga 3d. (Fleszar et. al proposed a construction for pseudopotentials when core states are not pseudized³².) Supposing the core were confined to the augmentation sphere at site R , we can eliminate all contributions to the matrix element $\langle \tilde{M}_I^{\mathbf{q}} \Psi_{\mathbf{k}n} | \Psi_{\mathbf{q}+\mathbf{k}n'} \rangle$ except from the product-basis contribution at R . Since also the augmented part of Ψ depends rather weakly on φ_{Rl} we can neglect the φ_{Rl} contribution to the eigenfunctions and assume that $\langle \tilde{M}_I^{\mathbf{q}} \Psi_{\mathbf{k}n} | \Psi_{\mathbf{q}+\mathbf{k}n'} \rangle$ only depends n, n', \mathbf{k} , or $\mathbf{k} + \mathbf{q}$ through the coefficients, $(\alpha_{Ru}^{\mathbf{k}n})^* \alpha_{Ru}^{\mathbf{k}+\mathbf{q}n'}$. Moreover, the core level energy is large and negative, and nearly independent of \mathbf{k} or n . Since the dominant contributions to D will come from coupling to low-lying states, we can approximate $\varepsilon_{kn} - \varepsilon_{k'n'}$ by a constant, e.g. $\varepsilon_F - \varepsilon_{\text{core}}$. These approximations are all modest but can vastly simplify the computation of

D^{Core} .

The fact that the core spills out slightly from the augmentation region needs to be taken into account¹⁴. This can readily be accomplished by integrating the core and corresponding valence φ_l to a larger radius, and orthogonalizing φ_l to the core (small nonorthogonality between φ_l and the core state seem to be the dominant source of error in the present core treatment.) Checks show that the adjustment to ϕ_l is small unless the core is very shallow, in which case the core should be treated as a valence state.

V. REMARKS ON THE PSEUDOPOTENTIAL APPROXIMATION

As we noted in the introduction, use of pseudopotentials can substantially simplify the computational effort; however, the use of pseudopotentials is less well justified in GW theory than in the LDA. Broadly speaking, QP levels from pseudopotential calculations tend to be higher than corresponding all-electron results. We should consider the following points.

1. Need for a pseudopotential not constructed from the LDA;
2. Need for a constraint to justify the use of a PP-derived Σ .

All-electron methods that properly subtract $V_{\text{xc}}^{\text{LDA}}$ calculated from the full density are in reasonable agreement with each other^{3,7,18,26,33}; those that subtract valence density only^{4,5} are also in reasonable agreement for cases such as Si and SiC where the cores are sufficiently deep. Moreover, core contributions should be rather modest, as we have shown, provided that the Fock exchange is included properly. Our own experience using all-electron methods suggests that the LDA treatment of core levels, where QP levels are computed from Eq. (18), will be problematic for GW ⁷ unless the cores are very deep. Since a pseudopotential construction is an approximation whose justification is grounded in an all-electron theory, we can expect GW calculations based on an LDA pseudopotential should be similarly problematic. There is apparently a significant dependence on how cores are treated in PP implementations^{30,32,34}, even in Si with its deep $2p$ cores; see for example, inset in Fig. 2 (A reliable comparison of literature values is difficult since it is not clear how well converged different calculations are within the PP approximation, such as choice of cutoff in n' , choice of k -mesh, as we describe below.)

As we have seen, exchange-only (Hartree-Fock) treatment of core states is often not such a bad approximation; moreover it should be possible to incorporate the dominant RPA

contributions from shallow cores as we discussed in the previous section. This suggests that it may be possible to construct reliable HF-based pseudopotentials. There may be, however, some difficulties. HF theory is a very poor descriptor of the electronic structure in solids, so using straight HF-derived $\Psi_{\mathbf{k}n}(\mathbf{r})$ and $\varepsilon_{\mathbf{k}n}$ to generate G and W will be similarly problematic. Better that the LDA potential should be used to make the $\Psi_{\mathbf{k}n}(\mathbf{r})$ and $\varepsilon_{\mathbf{k}n}$. However, such a construction would mean that $\Psi_{\mathbf{k}n}(\mathbf{r})$ and $\varepsilon_{\mathbf{k}n}$ are generated by a potential that puts core and valence on an inconsistent footing.

Shirley and co-workers were the first to apply Hartree-Fock-derived pseudopotentials³¹; they subsequently calculated QP levels in Si, GaAs and Ge using them, including at the same time some approximate contributions to the polarization³⁰. QP levels calculated this way move closer to all-electron results (compare Fig. 3 and Table II to Table IV in Ref. 30). It would be instructive to see to what extent calculations based on HF pseudopotentials, with and without core polarization contributions, can separately reproduce the HF and full GW QP levels in Table II.

In cases where the highest cores are put explicitly into the valence^{8,32} there is reasonable agreement between PP and all-electron results: Tiago's and the present all-electron calculation of the X_{1c} level in Si are compared in Fig. 2. There is agreement between the two methods at the ~ 0.1 eV level in Si³⁵ and similar agreement is found for GaAs and Ge, with the PP results systematically higher than all-electron results by $\sim 0-0.1$ eV (compare Tiago's paper to Table II). Precise comparison is somewhat difficult, in part because Tiago's calculation used a very large LDA basis, and therefore it would seem that the PP data in the inset of Fig. (2) *should* be extrapolated to $1/n' \rightarrow 0$. Moreover, it is possible that Tiago's calculation suffers from incomplete k -convergence. Both PP calculations presented in Fig. 2 used a $4 \times 4 \times 4$ k -mesh. k -convergence is mainly controlled by the $1/k^2$ divergence in the exchange near Γ . If the k -convergence in the PP calculation is similar to our experience with the offset- Γ method^{5,36}, much of the remaining discrepancy in the Tiago's and our present calculations can be attributed to it²⁰. It is similarly problematic to compare Tiago's calculation to the HF-PP + core polarization calculation by Shirley et. al³⁰ (where a finer k mesh was used to calculate D).

Fleszar et al.³² calculated $G^{\text{LDA}}W^{\text{LDA}}$ QP levels for a variety of II-VI semiconductors, including the highest s and p cores in the valence. Their values are also in reasonable agreement with all-electron results presented in Table III (below), though the PP calculations are

systematically higher by $\sim 0.0\text{--}0.2$ eV. (Part of the discrepancy can be traced to contributions from high-lying d electrons, which are included in the present calculation using local orbitals.) Even when the high-lying s and p core states are included explicitly in the valence, it still seems to be the case that PP calculations of QP levels of conduction bands in semiconductors are systematically slightly larger by ~ 0.1 eV than the all-electron calculations predict.

Considering the various possible difficulties in PP constructions for GW , and the ~ 0.1 eV uncertainty in the all-electron calculations²², the agreement between all-electron and PP $G^{\text{LDA}}W^{\text{LDA}}$ calculations which treat the high-lying core states as valence, appears to be reasonable.

The norm conservation condition ensures that the Hartree potential is reasonably evaluated in a PP calculation. Because the charge conserved, the Hartree potential V^H and energy $1/2\int n(\mathbf{r})V^H(\mathbf{r})d\mathbf{r}$ are reasonably described. It is well established the LDA eigenvalues and (pseudo)eigenfunctions are good replacements for their all-electron counterparts. These means that the (pseudo)density-density response function Eq. (16) should be reasonable, and so should the (pseudo) $W(\mathbf{r}, \mathbf{r}')$.

However, there is no corresponding condition that ensures the self-energy iGW reasonably approximates the all-electron counterpart. (Even in the LDA, “nonlinear core correction” terms in the exchange-correlation potential are often added to PP results more reliable.) Thus there is some uncertainty about the validity of the PP construction for GW , even one based on Hartree-Fock theory. The discrepancy becomes particularly pronounced when comparing self-consistent GW results. Different kinds of self-consistent all-electron calculations^{3,26}, produce rather similar results in the few cases where a comparison can be made (although the self-consistency was done differently in the two cases). Self-consistent PP and all-electron results, however, are radically different^{3,37}, with the PP gap in Si drastically larger than the experimental value. It may be possible to introduce some kind of constraint for some average property of the density matrix, corresponding to the norm conservation condition for the density, which will help to ensure that at least the exchange potential or GW^{static} is reliable (which is the dominant part of the self-energy). Inclusion of such a constraint may improve the reliability of PP’s for GW .

Shirley and co-workers offer some *a posteriori* justification that Hartree-Fock derived PP’s can reasonably describe properties of free atoms and small molecules^{28,31}; Delaney could find

a similar justification for the Be atom². While PP's derived in this way *may* be transferable to the solid, it should be noted that the dielectric response in solids is radically different from small molecules. Consequently, establishing that PP's are transferable in small molecules is not by itself sufficient to justify the transferability to the solid case. Systematic checks are needed to establish their validity, much as occurred in the early days of constructing PP's for the LDA.

VI. $G^{\text{LDA}}W^{\text{LDA}}$ APPROXIMATION

Delaney's second claim argues that $G^{\text{LDA}}W^{\text{LDA}}$, i.e. GW whose self-energy is constructed from the LDA potential, is an adequate (or better) approximation than self-consistent GW . Delaney showed it to be the case in the Be atom. But dielectric response of free atoms is small, and W is poorly screened. Consequently a perturbation expansion in powers of W is less justified than in a solid where the screening is much stronger. For solids it is typically not true that $G^{\text{LDA}}W^{\text{LDA}}$ is a good, or even adequate approximation. Even in very simple materials such as *sp* semiconductors, $G^{\text{LDA}}W^{\text{LDA}}$ bandgaps are *always* underestimated when properly calculated^{7,32}. This can be rather easily understood because the starting gaps are too small, resulting in W being screened too strongly.

Before turning to some specific examples, there is an important formal consideration, namely the role of the Z factor entering into Eq. (6). It enters in the standard theory through the energy-dependence of Σ . In the language of perturbation theory Eq. (6) is a perturbation where Σ should be evaluated at the QP level $E_{\mathbf{k}n}$. But in practice Σ is evaluated at the LDA energy $\varepsilon_{\mathbf{k}n}$, and the Z factor is designed to correct for this error. This is because E_{kn} is defined as the peak of the spectral function $A(k, \omega) = \pi^{-1}|\text{Im}(G(k, \omega))|$ along the real ω axis. In the $G^{\text{LDA}}W^{\text{LDA}}$ construction,

$$G(k, \omega) = \frac{1}{\omega - \varepsilon_k - \Sigma(k, \omega)} \quad (20)$$

the poles of G correspond to

$$\begin{aligned} 0 &= E_k - \varepsilon_k - \text{Re}\Sigma(k, E_k) \\ &\approx E_k - \varepsilon_k - \text{Re}\Sigma(k, \varepsilon_k) - \frac{\partial \Sigma}{\partial \omega}(E_k - \varepsilon_k) \end{aligned} \quad (21)$$

which leads to Eq. (6).

On the other hand, Niquet and Gonze³⁸ calculated the interacting bandgap energy (within RPA) to obtain a correction to the Kohn-Sham bandgap energy, and found that the difference is essentially Eq. (6) with $Z = 1$. We offer another justification here for the use of $Z = 1$.

We can compare two kinds of self-energy: $\Sigma(k, E_k, [G])$ and $\Sigma(k, E_k, [G^{\text{LDA}}])$, where G in the former case includes a limited form of self-consistency. Eq. (6) is the result of $\Sigma(k, E_k, [G^{\text{LDA}}])$. We can obtain an approximate self-consistency by updating the eigenvalues entering into G but retaining the LDA eigenfunctions: this corresponds to (i) approximating $\Sigma_{nn}(k, \omega)$ by the static $\Sigma_{nn}(k, E_{kn})$, and (ii) discarding the off-diagonal $\Sigma_{n \neq n'}$.

Consider a two-states model whose LDA eigenvalues and eigenfunctions are given by ψ_1, ε_1 , and ψ_2, ε_2 , and the Fermi energy falls between these states: $\varepsilon_2 > E_F > \varepsilon_1$. Then the LDA Green's function is

$$G^{\text{LDA}}(\omega) = \frac{|\psi_1\rangle\langle\psi_1|}{\omega - \varepsilon_1 - i\epsilon} + \frac{|\psi_2\rangle\langle\psi_2|}{\omega - \varepsilon_2 + i\epsilon}. \quad (22)$$

and the self-consistent one is the same, except for some shifts of the eigenvalues:

$$G(\omega) = \frac{|\psi_1\rangle\langle\psi_1|}{\omega - E_1 - i\epsilon} + \frac{|\psi_2\rangle\langle\psi_2|}{\omega - E_2 + i\epsilon}. \quad (23)$$

E_1 is given by

$$E_1 = \varepsilon_1 + \text{Re}\langle\psi_1|\Sigma(E_1, [G]) - V_{\text{xc}}^{\text{LDA}}|\psi_1\rangle \quad (24)$$

and a similar equation applies for E_2 .

If we further suppose that W is well described by the LDA; i.e., it does not change as we iterate to self-consistency, and only the diagonal elements $W_1(\omega) = \langle\psi_1\psi_1|W(\omega)|\psi_1\psi_1\rangle$ and $W_2(\omega) = \langle\psi_2\psi_2|W(\omega)|\psi_2\psi_2\rangle$ are important, Σ becomes

$$\begin{aligned} \text{Re}\langle\psi_1|(\Sigma(E_1, [G]))|\psi_1\rangle &= \text{Re} \int \langle\psi_1|iG(E_1 + \omega')W(\omega')|\psi_1\rangle d\omega' \\ &\approx \text{Re} \int \frac{iW_1^{\text{LDA}}(\omega') d\omega'}{E_1 + \omega' - E_1 - i\epsilon} \\ &= \text{Re} \int \frac{iW_1^{\text{LDA}}(\omega') d\omega'}{\varepsilon_1 + \omega' - \varepsilon_1 - i\epsilon} \\ &= \text{Re}\langle\psi_1|\Sigma(\varepsilon_1, [G^{\text{LDA}}])|\psi_1\rangle \end{aligned} \quad (25)$$

A similar equation applies for E_2 . The energy shift $\epsilon \rightarrow E$ entering into the evaluation Σ is exactly compensated by the energy shift in $G^{\text{LDA}} \rightarrow G$, or equivalently using $Z = 1$ is an

TABLE III: Fundamental gap, in eV. (For Gd, QP levels correspond to the position of the majority and minority f levels relative to E_f .) Low temperature experimental data were used when available. QP levels are calculated in the traditional perturbation theory, Eq. (7). Also shown are results when Z is taken to be unity. An $8 \times 8 \times 8$ k -mesh was used for the cubic semiconductors; a wurtzite semiconductors were calculated with a $6 \times 6 \times 6$ mesh (a w preceding a compound means the material was calculated in the wurtzite structure). $G^{\text{LDA}}W^{\text{LDA}}$ calculations leave out spin-orbit coupling and zero-point motion effects. The former is determined from $\Delta/3$, where Δ is the spin splitting of the Γ_{15v} level (in the zincblende structure); it is shown in the “ $\Delta/3$ ” column. Contributions to zero-point motion are estimated from Table 2 in Ref. 39 and are shown in the “ZP” column. The “adjusted” gap adds these columns to the true gap, and is the appropriate quantity to compare to GW .

	LDA $G^{\text{LDA}}W^{\text{LDA}}$ ($Z = 1$)		Expt	$\Delta/3$	ZP	Adj	
C	4.09	5.48	5.74	5.49	0	0.34	5.83
Si	0.46	0.95 ^a	1.10	1.17	0.01	0.06	1.24
Ge	-0.13	0.66	0.83	0.78	0.10	0.05	0.93
GaAs	0.34	1.40	1.70	1.52	0.11	0.10	1.73
wAlN	4.20	5.83	6.24	6.28	0 ^b	0.20	6.48
wInN	-0.24	0.17 ^a	0.30	0.69	0 ^b	0.16	0.85
wZnO	0.71	2.42	2.95	3.44	0 ^b	0.16	3.60
ZnS	1.86	3.21	3.57	3.78	0.03	0.10	3.91
ZnSe	1.05	2.25	2.53	2.82	0.13	0.09	3.04
ZnTe	1.03	2.23	2.55	2.39	0.30	0.08	2.77
CuBr	0.29	1.56	1.98	3.1	0.04	0.09 ^c	3.23
CdO	-0.56	0.10	0.22	0.84	0.01 ^b	0.05	0.90
wCdS	0.93	1.98	2.24	2.50	0.03	0.07	2.60
SrTiO ₃	1.76	3.73	4.42	~3.3			
NiO	0.45	1.1	1.6	4.3			
CoO	0	0	0	6.0			
Gd $^\uparrow$	-4.5	-5.5	-6.0	-7.9			
Gd $^\downarrow$	0.3	0.2	1.6	4.3			

^aSee Ref. 35

^bLDA calculation

^cEstimated from ZnSe

approximate way to obtain self-consistency. Eq. (25) corresponds Eq. (6) with $Z = 1$. Table III presents some $G^{\text{LDA}}W^{\text{LDA}}$ results both with and without the Z factor.

Table III confirms our earlier claim⁷ that bandgaps in simple sp semiconductors are always underestimated. Similar results are found in Ref. 32 for II-VI compounds. Results with $Z = 1$ are significantly better, but they continue to be too small. It can happen that $G^{\text{LDA}}W^{\text{LDA}}$ can produce gaps in good agreement with experiment, for the wrong reason: SrTiO_3 is probably such a case. The LDA underestimates the gaps rather less than in, e.g., AlN with a similar dielectric constant ($\epsilon_\infty \sim 5$). Both materials suffer from the standard deficiency in the LDA, namely the omission of a highly nonlocal (screened) exchange which is mainly responsible for the ubiquitous gap underestimate in sp semiconductors⁴⁰. But the lowest conduction bands of SrTiO_3 are rather narrow bands of d character, which are susceptible to electron-hole correlation effects missing in the RPA (and LDA). The missing excitonic-like contributions to D means that the RPA under-screens W , which consequently results in the gap being overestimated. But in the LDA these two errors cancel somewhat better in SrTiO_3 than they do in AlN, resulting in fortuitously good LDA and $G^{\text{LDA}}W^{\text{LDA}}$ gaps.

In general, $G^{\text{LDA}}W^{\text{LDA}}$ errors are rather closely tied to the quality of LDA starting point. In the covalent sp semiconductors C, Si and Ge, $G^{\text{LDA}}W^{\text{LDA}}$ gaps are rather good for $Z = 1$. In the series $\text{Zn}(\text{Te,Se,S,O})$, the deviation between the LDA and experimental gap steadily worsens, and so does the $G^{\text{LDA}}W^{\text{LDA}}$ gap. For ZnO , and even more so in CuBr , the $G^{\text{LDA}}W^{\text{LDA}}$ gap falls far below experiment. For these simple sp materials there is a close link between the $G^{\text{LDA}}W^{\text{LDA}}$ error and the strength of the dielectric response ϵ . When ϵ is large, the LDA is a rather better starting point than when it is small: the nonlocal exchange is less well screened for small ϵ , so its omission from the LDA generates somewhat larger errors in the $\Psi_{\mathbf{k}n}$ and $\varepsilon_{\mathbf{k}n}$, and correspondingly larger errors in the $G^{\text{LDA}}W^{\text{LDA}}$ QP levels.

Discrepancies between $G^{\text{LDA}}W^{\text{LDA}}$ and experiment become drastic when correlations are strong. E_g for the highly correlated NiO is far from experiment and E_c falls at the wrong place (between Γ and X). As Table III shows, the LDA puts f levels in Gd too close to ε_F . $G^{\text{LDA}}W^{\text{LDA}}$ results are only moderately better: shifts in the Gd f level relative to the LDA are severely underestimated (see Table I). The LDA fails even qualitatively in CoO : it predicts a metal with ε_F passing through an itinerant band of d character. $G^{\text{LDA}}W^{\text{LDA}}$ does not exchange-split this band into a pair of well-separated levels as it should, with the result

that $G^{\text{LDA}}W^{\text{LDA}}$ QP levels in CoO are essentially similar to the LDA. Similar problems occur with ErAs: the LDA predicts a very narrow minority f band straddling the Fermi level, whereas in reality the minority f manifold is exchange-split into several distinct levels well removed from ε_F ⁴¹. $G^{\text{LDA}}W^{\text{LDA}}$ shifts the minority f levels only slightly relative to the LDA: the entire f manifold remains clustered in a narrow band at the Fermi level, appearing once again qualitatively similar to the LDA.

Generally speaking, the $G^{\text{LDA}}W^{\text{LDA}}$ approximation is reasonable only under limited circumstances—when the LDA itself is already reasonable. Crudely speaking the LDA errors in the sp materials originate from lack of nonlocality in $V_{\text{xc}}^{\text{LDA}}$ of itinerant electrons—the nonlocality is spread out over many neighbors. As for correlations in d and f systems, the predominant LDA errors originate from the lack of nonlocality between orbitals of a particular l character within a site. A more realistic description of the potential has a (screened) Hartree-Fock-like, orbital-dependent exchange between the different orbitals within a particular d or f channel at a particular site. LDA+ U theory adds an orbital-dependent exchange to the LDA of this type (nonlocality restricted to orbitals of a particular l within a site), which enables it to account for this latter kind of error—albeit in an *ad hoc* manner. LDA+ U at least qualitatively remedies the rather dramatic failures in CoO⁴² and ErAs⁴¹. As we will show elsewhere, $G^{\text{LDA}+U}W^{\text{LDA}+U}$ QP levels, where G and W are constructed from an LDA+ U potential, *do* generate reasonable results for ErAs and CoO. But in this case the $G^{\text{LDA}+U}W^{\text{LDA}+U}$ QP levels depend rather sensitively on the choice of U , which means we can not regard such a method as *ab initio*.

A second fundamental problem in $G^{\text{LDA}}W^{\text{LDA}}$ is connected with the fact that it is not a conserving approximation⁴³. Lack of charge conservation leads to ambiguities in the interpretation of the QP levels, as well as integrated quantities such as the magnetic moment. In simple semiconductors this is not particularly important, but in metallic systems the effect can be dramatic. MnAs offers a clear example of the ambiguity: it is a spin-polarized material in the NiAs phase with a magnetic moment of $3.4\mu_B/\text{Mn atom}$. The LDA predicts a moment of $3.0\mu_B/\text{Mn atom}$, which reflects the tendency of the LDA to place the majority d levels too shallow, and to underestimate the majority-minority spin splitting. Fig. 4 compares some LDA energy bands (dotted lines) to $G^{\text{LDA}}W^{\text{LDA}}$ calculations. Majority LDA d levels occupy a narrow band between $\varepsilon_F - 4$ eV and $\varepsilon_F - 1$ eV; the corresponding minority levels fall predominantly between ε_F and $\varepsilon_F + 3$ eV. Straightforward application of the 1-shot

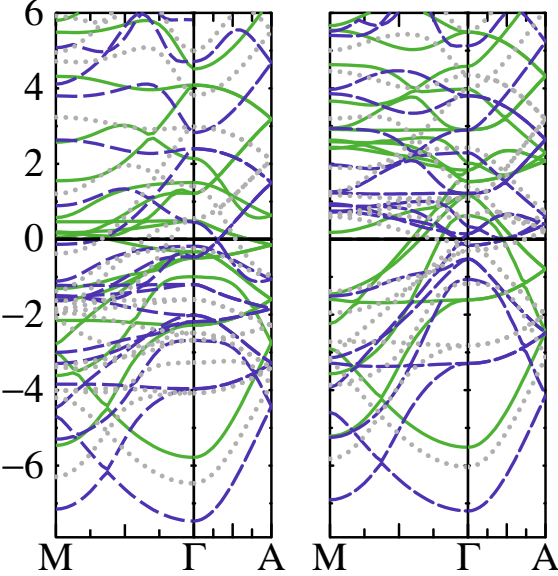


FIG. 4: $G^{\text{LDA}}W^{\text{LDA}}$ calculations of the energy bands of MnAs in the NiAs structure (eV). Left panels are for majority spin; right panels for minority spin. The entire matrix $\Sigma_{nn'}$ is included, and no Z factor is used. In the diagonal approximation $\Sigma_{nn'} \approx \Sigma_{nn} \delta_{nn'}$ this would correspond to Eq. (6) with $Z = 1$. Light dotted lines: LDA bands. Dark solid lines: $G^{\text{LDA}}W^{\text{LDA}}$ adding $\Sigma - V^{\text{xc}}$ to the LDA potential and the LDA Fermi level. Dark dashed lines: same bands but shifted to the Fermi level as determined from the charge neutrality point corresponding to the $\Sigma - V^{\text{xc}}$ potential.

formula Eq. (6) with $Z = 1$ yields the dark solid bands in Fig. 4. (The calculation does not precisely correspond to Eq. (6) because the full nondiagonal $\Sigma_{nn'}$ was included.) Majority and minority Mn d levels all shift up in energy, to a window $(\varepsilon_F - 2, \varepsilon_F + 1)$ eV for majority and $(\varepsilon_F + 2, \varepsilon_F + 5)$ eV for minority bands. If we take ε_F to be fixed, charge is not conserved: as a result there is a charge deficit of 6.0 electrons and the magnetic moment shrinks to $1.1\mu_B/\text{atom}$. It is apparent that the sp bands also shift by $\sim +0.6$ eV (compare levels near -6 eV or $+4$ eV at Γ).

We can shift ε_F to conserve charge, which puts the new ε_F 1.6 eV higher than in the LDA case. (The dark dashed lines show the $G^{\text{LDA}}W^{\text{LDA}}$ bands shifted by -1.6 eV.) The d band positions again become reasonable: they shift roughly back to where the LDA put them with a slight increase in majority-minority splitting. Consequently the magnetic moment is reasonable ($3.15\mu_B$). But now itinerant bands of sp character are unphysically shifted down relative to the LDA, by ~ 1.1 eV. Thus, $G^{\text{LDA}}W^{\text{LDA}}$ fails rather badly at predicting the relative position of the s and d centers of gravity. In any case it is clear that such large

redistribution of the occupation of QP levels will result in sizeable shifts of the electron density, which calls into question the validity of the 1-shot approach altogether.

To summarize, one-shot GW approaches are rather unsatisfactory in general. We have seen that the LDA potential is adequate to construct G and W only under limited circumstances. Since one-shot GW is quite sensitive to the generating potential, in a sense it cannot be considered truly *ab initio*. Some kind of self-consistency is essential: the generating potential should be a functional of Σ so that the results are not artifacts of external conditions. True self-consistent GW is one possibility: it is internally consistent, and it is conserving. However, there are difficulties with this approach: bandwidths in the homogeneous gas are rather significantly overestimated⁴⁴. The loss of QP weight is substantial if G is iterated to true self-consistency within the RPA, as was established by Bechstedt et al⁴⁵. We have argued previously that this loss results in a rather poor G and we have proposed an alternate construction²⁶. As we will show elsewhere¹³, there is a formal justification for such a construction; moreover, it produces a consistently reliable approach for the calculation of QP levels in broad classes of solids, including all of the compounds discussed in this paper. Equally significantly (in contrast to one-shot approaches such as $G^{\text{LDA}}W^{\text{LDA}}$), the remaining errors are small and highly systematic.

VII. CONCLUSIONS

To conclude, we have analyzed various possible sources of error in implementations of the GW approximation, using calculations based on an all-electron method with generalized Linear Muffin Tin Orbitals as a basis.

The discrepancy in convergence rates between a prior all-electron and a pseudopotential calculation could be partially resolved. We then presented a different analysis of convergence that is of particular importance for minimal-basis implementations, and argued that traditional measures (as given in Figs. 1 and 2) can be misleading. A finite size basis truncates the full Hilbert space of eigenfunctions in a different way than the truncation embodied in Figs. 1 and 2; and we showed that a suitably constructed minimal basis is sufficient to precisely describe QP levels within 1 Ry or so of the Fermi level. We also showed that traditional linearization of basis functions, either explicit in an all-electron method or implicit through the construction of a pseudopotential, result in errors approximately independent of the size

of basis. Addition of local orbitals to extend the linear approximation results in modest shifts in *sp* nitride and oxide compounds, and shifts of order 1-2 eV in transition-metal oxides and rare earths elements.

We analyzed core contributions to the self-energy, and showed that a Hartree-Fock treatment of the core is adequate in most cases. For all but the most shallow cores (such as Na 2*p* and Ga 3*d*), we showed that it is sufficient to include the core contribution to the polarization only; an approximate and rather painless implementation was suggested. These results can provide a framework for improved treatment of the core within a pseudopotential approximation.

Last we considered the validity of the one-shot $G^{\text{LDA}}W^{\text{LDA}}$ approximation. A “conventional wisdom” that sc*GW* is worse than $G^{\text{LDA}}W^{\text{LDA}}$ had evolved from two papers: Holm and von Barth’s demonstration⁴⁴ that bandwidths in the homogeneous gas are overestimated, and Schöne and Eguiluz’s pseudopotential sc*GW* calculation⁴⁶ that predicted the Si bandgap was severely overestimated in Si. The former appears to be real; the latter however, appears to be an artifact of the pseudopotential approximation. We showed that $G^{\text{LDA}}W^{\text{LDA}}$ results in systematic errors, sometimes modest, and at other times drastic, depending on reasonableness of the starting Green’s function. We presented an argument that using $Z=1$ accounts in an approximate way for the neglect of self-consistency; we showed for simple *sp* systems the systematic errors can be partially mitigated through the omission of the Z factor.

This work was supported by ONR contract N00014-02-1-1025. S.F. was supported by DOE, BES Contract No. DE-AC04-94AL85000.

¹ L. Hedin, Phys. Rev. **139**, A796 (1965).

² K. Delaney, P. García-González, A. Rubio, P. Rinke, and R. Godby, Phys. Rev. Lett. **93**, 249701 (2004).

³ W. Ku and A. G. Eguiluz, Phys. Rev. Lett. **89**, 126401 (2002).

⁴ N. Hamada, M. Hwang, and A. J. Freeman, Phys. Rev. B **41**, 3620 (1990), URL <http://link.aps.org/abstract/PRB/v41/p3620>.

⁵ S. Lebegue, B. Arnaud, M. Alouani, and P. Bloechl, Phys. Rev. B **67**, 155208 (2003).

⁶ There have been a few all-electron implementations of the *GW* method; however, some of them treat the core at the LDA level, and subtract the valence-only part of the LDA exchange correlation potential⁵. Thus, care must be taken when comparing different all-electron calculations. In the Si and SiC cases the cores are very deep, and it matters little whether only the valence electrons or all the electrons are included in the *GW* potential.

⁷ T. Kotani and M. van Schilfgaarde, Sol. State Commun. **121**, 461 (2002).

⁸ M. L. Tiago, S. Ismail-Beigi, and S. G. Louie, Phys. Rev. B **69**, 125212 (2004).

⁹ M. Methfessel, M. van Schilfgaarde, and R. A. Casali, in *Lecture Notes in Physics*, edited by H. Dreyssse (Springer-Verlag, Berlin, 2000), vol. 535.

¹⁰ O. K. Andersen, Phys. Rev. B **12**, 3060 (1975).

¹¹ E. Bott, M. Methfessel, W. Krabs, and P. C. Schmidt, J. Math. Phys. **39**, 3393 (1998).

¹² P. E. Blochl, Phys. Rev. B **50**, 17953 (1994).

¹³ T. Kotani, M. van Schilfgaarde, and S. Faleev (2005), in preparation.

¹⁴ In the *GW* scheme as we have currently implemented it, core states are approximated by truncating them outside the MT spheres, and scaling the part inside the MT sphere to conserve charge. Alternatively, the core wave function can be obtained subject to the boundary condition that the value and slope vanish at the MT boundary. In either case, the core is not orthogonal to the valence; this appears to be the primary source of error in the present treatment of the core.

¹⁵ In the LDA a small amount of the envelope function remains inside the augmentation spheres, to handle incomplete l convergence of the augmentation functions. In the present *GW* implementation this feature is not retained, because of the nonlocal character of the potential. As a consequence wave function products must be augmented to higher l than in the LDA case.

¹⁶ F. Aryasetiawan and O. Gunnarsson, Phys. Rev. B **49**, 16214 (1994).

¹⁷ M. Usuda, N. Hamada, T. Kotani, and M. van Schilfgaarde, Phys. Rev. B **66**, 125101 (2002).

¹⁸ C. Friedrich, A. Schindlmayr, S. Blugel, and T. Kotani, in preparation.

¹⁹ J. Rath and A. Freeman, Phys. Rev. B **11**, 2109 (1975).

²⁰ Using the linear tetrahedron method, a mesh of $6 \times 6 \times 6$ divisions (doubling the number of points in the energy denominator) overestimated the k -converged result by ~ 0.02 eV in Si, while a $4 \times 4 \times 4$ mesh overestimated the k -converged result by ~ 0.10 eV. These shifts were approximately unchanged when varying, e.g., the basis set or the number of unoccupied states.

²¹ W. Ku and A. G. Eguiluz, Phys. Rev. Lett. **93**, 249702 (2004).

²² A recent LAPW-GW calculation by C.Friedrich, A.Schindlmayr, S.Blügel and T.Kotani (in preparation), including eigenfunctions with about 300 valence bands, obtained a bandgap slightly larger (by ~ 0.04 eV) than the results presented here, when similar input conditions for the *GW* calculation are used.

²³ L. Steinbeck, A. Rubio, L. Reining, M. Torrent, I. White, and R. Godby, Computer Physics Communications **125**, 105 (2000).

²⁴ G. B. Bachelet, D. R. Hamann, and M. Schlüter, Phys. Rev. B **26**, 4199 (1982).

²⁵ O. K. Andersen, T. Saha-Dasgupta, R. W. Tank, and G. K. C. A. O. Jepsen, in *Lecture Notes in Physics*, edited by H. Dreysse (Springer-Verlag, Berlin, 2000), vol. 535.

²⁶ S. V. Faleev, M. van Schilfgaarde, and T. Kotani, Phys. Rev. Lett. **93**, 126406 (2004).

²⁷ E. L. Shirley, L. Mitás, and R. M. Martin, Phys. Rev. B **44**, 3395 (1991).

²⁸ E. L. Shirley and R. M. Martin, Phys. Rev. B **47**, 15 (1993).

²⁹ E. L. Shirley, X. Zhu, and S. G. Louie, Phys. Rev. Lett. **69**, 2955 (1992).

³⁰ E. L. Shirley, X. Zhu, and S. G. Louie, Phys. Rev. B **56**, 6648 (1997).

³¹ E. L. Shirley, R. M. Martin, G. B. Bachelet, and D. M. Ceperley, Phys. Rev. B **42**, 5057 (1990).

³² A. Fleszar and W. Hanke, Phys. Rev. B **71**, 045207 (2005).

³³ M. Usuda, H. Hamada, K. Siraishi, and A. Oshiyama, Jpn. J. Appl. Phys. Lett. (part 2) **43**, L407 (2004).

³⁴ M. Rohlfing, P. Kruger, and J. Pollmann, Phys. Rev. Lett. **75**, 3489 (1995).

³⁵ QP levels calculated by ourselves in Ref. 7 did not have local orbitals included. Mostly for that reason, the QP levels are a little different from those cited here. Also, the gap in wurtzite InN cited here is 0.17 eV larger than the 0.02 eV reported by Usuda³³, who used LAPW eigenfunctions that did not have local orbitals. (Leaving out the N 3p and In 5d local orbitals, we obtained a gap of 0.01 eV with an LMTO basis in Ref. 7.) The basis sets used in the present calculations are substantially larger, and tolerances set tighter than in what Ref. 7 used. These changes make additional corrections of ~ 0.05 eV. Finally the fundamental gap for Si was incorrectly tabulated as 0.84 eV in Ref. 26: the actual value for the basis used in that paper was 0.91 eV.

³⁶ A.Yamasaki and T.Fujiwara, J. Phys. Soc. Japan **72**, 607 (2003).

³⁷ W. D. Schöne and A. G. Eguiluz, Phys. Rev. Lett. **81**, 1662 (1998).

³⁸ Y. M. Niquet and X. Gonze, Phys. Rev. B **70**, 245115 (2004).

³⁹ F. Manjón, M. Hernández-Fenollosa, B. Mari, S. Li, C. Poweleit, A. Bell, J. Menéndez, and M. Cardona, Eur. Phys. B **40**, 453 (2004).

⁴⁰ E. G. Maksimov, I. I. Mazin, S. Y. Savrasov, and Y. A. Uspenski, J. Phys. C **1**, 2493 (1989).

⁴¹ T. Komesu, H.-K. Jeong, J. Choi, C. N. Borca, P. A. Dowben, A. G. Petukhov, B. D. Schultz, and C. J. Palmstrom, Phys. Rev. B **67**, 035104 (2003).

⁴² I. V. Solovyev, A. I. Liechtenstein, and K. Terakura, Phys. Rev. Lett. **80**, 5758 (1998).

⁴³ The usual terminology for “conserving approximation” refers to conservation in the Baym-Kadanoff sense: charge, energy and momentum are conserved when an external perturbation is applied. We are referring here to ambiguities resulting from initially occupied levels becoming unoccupied, and vice-versa.

⁴⁴ B. Holm and U. von Barth, Phys. Rev. B **57**, 2108 (1998).

⁴⁵ F. Bechstedt, K. Tenelsen, B. Adolph, and R. D. Sole, Phys. Rev. Lett. **78**, 1528 (1997).

⁴⁶ W.-D. Schöne and A. Eguiluz, Phys. Rev. Lett **81**, 1662 (1998).